International Journal of Energy and Environmental Science
2017; 2(4): 79-88
http://www.sciencepublishinggroup.com/j/ijees
doi: 10.11648/j.ijees.20170204.12

Multiple Inlets of Hot Air to Drying Chamber of an Indirect Solar Dryer to Achieve Uniform Chamber Temperature

Mireya Ruiz Amelio*, Francisco Javier Altamirano García

Department of Engineering of Process and Hydraulics, Universidad Autónoma Metropolitana, Mexico City, Mexico

Email address:

myra@xanum.uam.mx (M. R. Amelio), paco.balam.akab@gmail.com (F. J. A. García)

*Corresponding author

To cite this article:

Mireya Ruiz Amelio, Francisco Javier Altamirano García. Multiple Inlets of Hot Air to Drying Chamber of an Indirect Solar Dryer to Achieve Uniform Chamber Temperature. *International Journal of Energy and Environmental Science*. Vol. 2, No. 4, 2017, pp. 79-88.
doi: 10.11648/j.ijees.20170204.12

Received: June 29, 2017; **Accepted**: July 12, 2017; **Published**: August 11, 2017

Abstract: The objective of this study is to obtain, by means of a new design of the pipe which transports the hot air from the solar collector to the drying chamber, a uniform temperature inside the drying chamber so that the product to be dried deposited in all trays is evenly dehydrated. Outdoor drying experiments of agricultural products were carried out to test the thermal performance of a natural convection solar dyer constructed. Almost all the products were dehydrated in a single day. Since the quality of dried product depends significantly on the temperature of the drying process passive thermography -was used to monitor the product temperature during the drying process. The thermal images reveal that under climatological normal conditions the temperature gradient is 1-3°C among the apple slices placed in trays; the existing moisture in the surface of the specimens is homogeneously released and the maximal temperature attained by the product is less than 40°C when the irradiance is 1000 W/m^2 and the average temperature of the hot air in the drying cabinet is 55°C.

Keywords: Indirect Type Solar Dryer, Solar Energy, Passive Thermography

1. Introduction

The process of dehydration is an important method for food preservation. In addition, the dried products take up less storage room, reduce transport weight and it is easier to pack them. Dehydration is the process to remove water from a product to transform it into a dry product in which the residual moisture is low. At the same time, the activity of water (a_w) is reduced ($a_w < 0.7$) below the level of the minimum activity for the development and reproduction of microorganisms (bacteria, yeasts and molds); besides, will inhibit chemical reactions of enzymatic degradation [1].

Nowadays food industries produce high quality dried products operated with commercial driers designed to use methods such as contact drying, convective drying, drying with radiation, dielectric drying, freezer drying, osmotic drying, microwave drying and vacuum drying. Among all these methods there is no one that provides a high-quality product at affordable cost. Energy consumption and product quality are critical parameters present in the selection of a drying process. The target of the food industry is to obtain a dry product with the desirable properties using less energy to subtract the moisture required [2]. Today, the convective drying method which operates with hot air flow is the most used [3].

During the drying process, it is essential to avoid undesirable changes affecting the quality of the dried products [4]. Some product properties depend on the structure which is changing during dehydration because the viscoelastic matrix is contracted due to pits that remain when the water is removed and causes shrinkage, cracks and porosity in the dried products [5]. When applying heat, it can change some physical and chemical properties of products such as loss of nutrients, taste, texture, color and rehydration capacity of the dried product [6]. If the drying is carried out at high temperature it is feasible to cause undesirable changes. The quality is improved if the process is operated at a lower temperature [7, 8] but then requires more operation time and is therefore expensive.

Temperature is one of the most important and frequently measured parameter in the food processes. In drying process, the temperature of product to be dried is commonly measured using a few probes: resistance temperature detectors,

thermocouples or thermistors. All these sensors have the disadvantage of being invasive i.e. in direct contact with the material and the monitoring of the temperature is made through measurements only at some points. From this information, it is not possible to make a reliable description of the temperature of all material placed in the tray. Measurements employing this method are limited in spatial and temporal resolutions. A recommended alternative is infrared (IR) thermography that is an image processing technique which transforms thermal radiation, emitted by any object with temperature above 0 Kelvin, into a visible image. A thermal imaging camera records the intensity of the radiation in the infrared of electromagnetic spectrum and turns it into a visible image: thermographic image. It offers immediately 2D visual information. It is easy to analyze the colored temperature distribution patterns.

The expensive dryers and the cost of fuels or electricity prevent them from being used by farmers in developing countries like Mexico. Many rural regions of Mexico have an important solar radiation practically during all year, so the use of solar energy can be a viable alternative to supply clean thermal energy for preserving the harvested products. Farmers can use natural convection solar dryers that operate without requiring power supplied by fossil fuels or by the electric grid, i.e. an environmental friendly technology at lower cost than other techniques of drying that reduce the environmental damages caused using fossil fuels.

In this paper is presented the design, construction, and thermal performance of an indirect solar dryer. It was tested with fruits and vegetables at the Universidad Autónoma Metropolitana in Mexico City (latitude 19.36° N, longitude 99.07° W, altitude 2235 m), although the dryer will be donated to a family farmer of Oaxaca. We carried out the dehydration of apple, strawberry, mango, tomato, nopal, mushroom, onion, and chili. The drying times for the different products were obtained. The drying process of agricultural products was monitored by passive thermography with the purpose of observing the temperature distribution on the slices' surface loaded in the trays, recording the maximal temperature reached by the product when the irradiance attains its maximum and detecting moisture content areas.

2. Drying and Solar Resource

Central Valleys of Oaxaca is a region in southwest Mexico where the solar resource is particularly abundant (6.04 KWh/m^2 daily on a 16.5^0 tilt surface). In this region, the main source of subsistence is the family agriculture. The local production is for self-consumption and for sale on the market as a fresh product. Using solar drying to convert perishable products into stabilized products that can be kept for a long-time and allows to access to other consumers and gives added value to this activity.

Figure 1 shows the average daily irradiance of each month for Santiago Jamiltepec Oaxaca, (latitude 16.5^0 N, longitude 98.3^0 W, altitude 80 m). From 10 a.m. to 12 noon and from 3 p.m. to 4 p.m. the average irradiance is at least greater than 500 W/m^2 and from 12 noon to 3 p.m. is between 800-990 W/m^2, so many products can be dehydrated in just one day.

Preserving agricultural products by open sun drying has been traditionally practiced since remote times in different parts of the world [9] but it has several disadvantages such as damaged products due to dust, rain and wind; insect infestation and loss by birds and animals. The poor quality and contamination of the products conducted to the search and development of alternative drying technologies [10]. Among the optional technologies, solar dryers provide a feasible option to produce quality dried products.

Fruits and vegetables require hot air in the temperature range of 45-60°C to keep their nutrients undamaged [11]. Dehydration is essentially a combined heat and mass transfer process. The moisture transport in food materials is complex since the internal structure is always changing. Initially, the heat is transferred to the solid surface and from there to inside. The moisture is transferred from inside to its surface as liquid and/or vapor and as steam is dragged by flowing air from its surface to the exterior.

3. Infrared Thermography

Temperature control and monitoring in food manufacturing process is essential to guarantee product quality during processes. IR thermography or thermal imaging is a non-invasive technique utilized for food quality and safety assessment in food industry [12]. In IR thermography, the thermal radiation emitted by a material is captured and transformed into a visible image of the temperature distribution of an object's surface. The surface temperature is mapped with high temporal and spatial resolution. Thermal imaging was initially developed for military purposes. Afterward, with technological advances in the processing of digitalized high- resolution images it has become a useful tool for other areas such as medicine, materials science, food, agriculture, and faire safety [13].

In 1800 William Herschel discovered the infrared radiation. In 1884 Josef Stefan and Ludwig Boltzmann showed that there is a correlation between the temperature of a body and the infrared radiation emitted. The amount of radiation emitted by an object is dependent on its temperature and emissivity. A thermal imaging camera records the intensity of the radiation in the infrared of the electromagnetic spectrum and displays it as a color thermal image, measures infrared radiation and calculates the temperature of the object. The calculation considers the emissivity of the surface of the measured object and reflected temperature compensation. Each pixel of the detector represents the temperature of a point and appears on the screen as a color image. Thermographic images show immediately 2D visual information by means the colored distribution temperature patterns without disturbing the drying process. The data can be recorded digitally and displayed instantly.

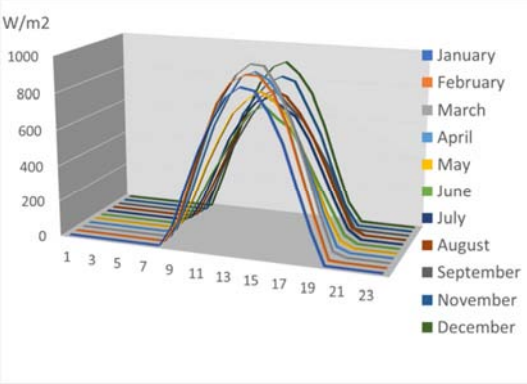

Figure 1. *Average daily irradiance of each month for Santiago, Oaxaca.*

There are two types of IR thermography systems: passive and active. In passive thermography, the images are obtained without application of external energy to the object. This type is usually employed for food's thermography during processing. The active thermography which requires application of thermal energy to the target before imaging is utilized to detect surface defects in foods [14, 15].

4. Solar Dryer Construction

A natural convection indirect type solar dryer was constructed and installed at the Universidad Autónoma Metropolitana in Mexico City. In this type of dryers, the solar rays do not strike directly on the material to be dried.

Figure 2. *Solar dryer.*

The solar dryer consists of a flat plate solar collector, an insulated drying chamber with a chimney for expelling air and a pipeline to conduct the hot air to the drying cabinet simultaneously at the bottom and at the side face opposite to the cabinet's door (figure 2). The collector length, width and height are 2 m, 0.8 m and 0.2 m respectively. The collector receives the energy of the sun and converts it into thermal energy raising the air temperature inside. It has a glass 0.4 cm thick that was used as transparent cover which allows the passage of the high-energy radiation coming from the sun but does not allow the passage of the low energy radiation coming from the inside of the collector. The radiation energy is captured by an absorber metallic plate painted with matte black color. Between the plate and the glass there are perforated plates to improve the transfer of heat to the air. The box is wood made painted matte black. The air enters through the front face that is covered by a mesh and leaves through three ducts that are in the rear face (figure 3).

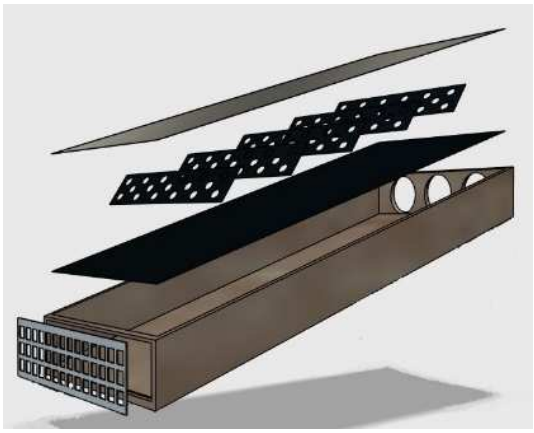

Figure 3. *Schematic view of solar collector.*

The pipelines that conduct the hot air from the collector to the drying cabinet are of polyvinyl chloride 0.15 m diameter. They were positioned in two different places: one at the center of the bottom and two, one on the right and one on the left on the face opposite to the door. Each of these has two reductions (5 cm diameter) and enters up and down as shown in figures 4 and 5, with the purpose that the product loaded in all the trays was uniformly dehydrated.

With the objective of constructing an economical dryer, a reused refrigerator was employed as a dryer cabinet. Its measures are 46 cm of length, 46 cm of width and 46 cm of height. It has an insulation material of 3 cm of thickness (figure 4).

The solar collector is oriented from north to south, free of shadowing effects and 20° tilted with respect to horizontal surface, this angle is function of the geographic location and it changes according to latitude.

5. Materials and Methods

Experiments were carried out with various fruits and vegetables like potatoes, tomatoes, pumpkins, onions, chili, mushrooms, mangoes, pineapples, strawberries, bananas, and apples in different meteorological conditions for eleven months to study the dryer performance. The procedure used with apples is described below. Fresh apples were obtained from a local market. They were washed, peeled and cut into uniform slices of 0.5 cm thick. The slices were immersed in a diluted solution of ascorbic acid for 5 minutes. They were immediately placed in the trays and put into the drying cabinet. The moisture content of samples before drying was determined by using an oven at 60°C until reaching a constant weight [16]. It has been found that the average initial moisture content is 83%.

Temperatures at different locations are measured using

NTC thermistors sensors which were connected to data logger system Smart Reader Plus 8 recorded at one-minute intervals and registered by the ACR TrendReader software. The sensors measured ambient air temperature, glass cover and plate collector temperature, air temperature at the inlet of the drying chamber and four more were fixed in its interior: in the middle, left side, right side and outlet area. Weight loss of sample during drying was measured using an electronic balance Ohaus. Irradiance on tilt plane was recorded by Energrid data logger that reads every 500 milliseconds and

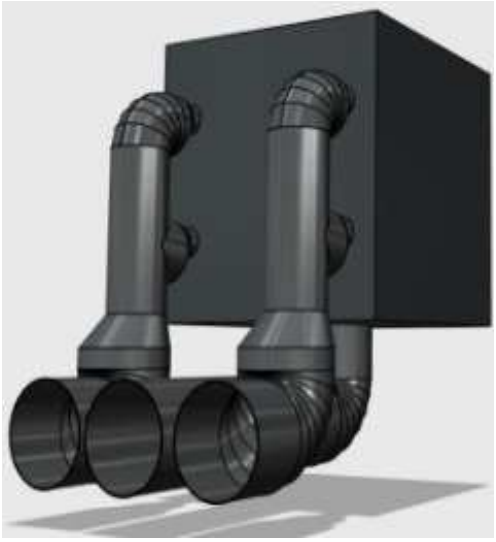

Figure 4. *Schematic view of drying chamber.*

Figure 5. *Drying chamber.*

records the average of these data, every 10 minutes and registered by Gridsoftware. Weather station WMR 300A recorded at one-minute intervals ambient temperature, wind speed, humidity, dew point, atmospheric pressure, and rainfall.

6. Image Acquisition

Thermal images had been obtained using passive thermography to monitoring drying process of apples with the purpose of observing the temperature distribution in the slices loaded on the trays, recording the maximum temperature reached by the product and detecting moisture content areas.

An infrared camera Fluke Ti 32 with a spectral infrared range of wavelength from 7.5 a 14mμ was mounted on the chimney allowing a free view of the top tray. The lens was positioned at an angle of 90º with respect to the surface under study. The non-cooled thermographic system achieves a geometric resolution of 320 x 240 IR pixels with a thermal resolution of 45 mK. The associated software SmartView has been used for processing the recorded infrared images.

7. Data Analysis

The change of moisture content in the time was determined by weighing the samples before and during the drying process at specific time intervals.

The initial moisture content on dry basis M_{0d} is defined as:

$$M_{0d} = (W_0 - W_d)/W_d \quad (1)$$

where W_0 is the initial weight of the product (kg), and W_d is the weight of the dried product (kg).

The initial moisture content on wet basis M_{0w} is defined as:

$$M_{0w} = (W_0 - W_d)/M_0 \quad (2)$$

The instantaneous moisture content M_t at any time t on dry basis is defined as:

$$M_t = (((M_{0d}+1)W_t)/W_0)-1 \quad (3)$$

where W_t is the weight of product at any time (kg).

The total mass of moisture evaporated from the product W_v is given by:

$$W_v = (M_t - M_f)W_d \quad (4)$$

where M_f is the is the final moisture content. The moisture ratio was obtained from the moisture content values using the next equation

$$MR = (M_t - M_e) / (M_i - M_e) \quad (5)$$

where MR is the dimensionless moisture ratio, M_t, M_0 and M_e are moisture content at any time t, initial moisture content and equilibrium moisture content (kg water/kg dry matter).

8. Results and Discussion

Experiments were carried out from June 2016 to April 2017 to characterize the thermal behavior of the solar dryer since the uniformity of hot air temperature inside the drying chamber is one of the objectives of this study and the reason for designing a different configuration to the usual which

introduces by the bottom of the drying chamber the hot air that comes from the solar collector.

8.1. Temperature Variation and Irradiance

Previous experiments done with this solar collector but in which the hot air was only introduced by the bottom of the drying chamber, showed temperature gradients that caused that the product deposited in all trays was not dried at the same time. The temperature in the drying chamber was uninterruptedly registered with unloaded chamber and loaded with the product to dry. Figures 6, 7, 8 and 9 show the irradiance, the temperature distribution of drying chamber, the temperature of the absorber plate, the collector glass cover and the ambient temperature. Figure 6 shows the temperature variation of the solar collector for seven consecutive days, from Monday to Saturday of the first week of January 2017; figure 7 corresponds to June 28, 2016 and shows the variation in temperature between the absorber plate and the hot air according to the radiation received. When the irradiance is close to 1000 W/m^2 a gradient of 30° is observed between the plate and the hot air; the average temperature of the plate reaches values of 87-88°C and the hot air of 57-58°C. When the irradiance is around 700 W/m^2 a 20°C gradient is observed. No more than 10°C is the gradient when the radiation is under 400 W/m^2; figure 8 displays the thermal performance of April 3, 2017. In this graph, the effects of the variability of the irradiance in the temperature reached by the components of the collector are observed. All these graphs were obtained with unload chamber. Figure 9 is from July 20, 2016 during the drying of mushrooms. Although, in this day is observed a notably variable radiation, with an average irradiation of 4.25 W/m^2, the mushrooms were dehydrated in just one day. According to these graphs the temperature reached by the absorber plate and consequently the one of the hot air obeys to variability of solar radiation that strikes the collector. Instantaneous temperature measured throughout the day has practically the same value in the different points inside the drying chamber. The temperatures of the cover and that of the air inside the drying chamber are similar.

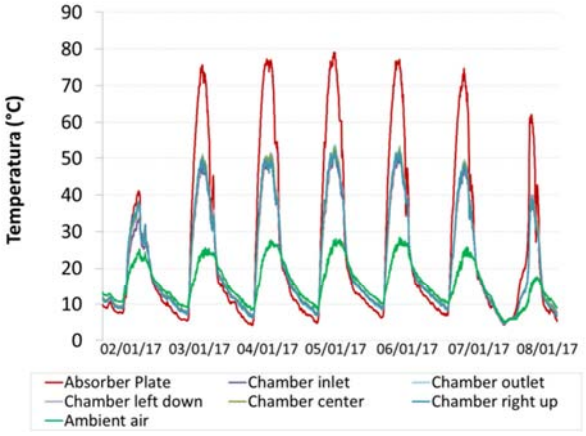

Figure 6. *Temperature distribution inside the drying chamber from January 2 to 8, 2017.*

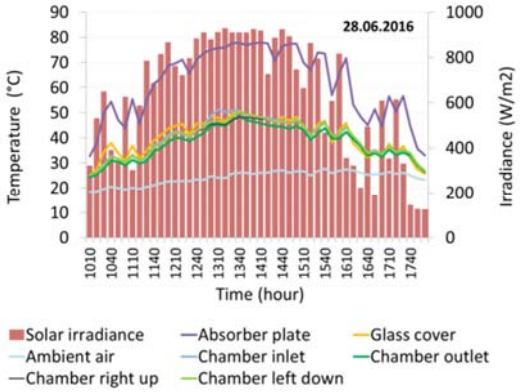

Figure 7. *Irradiance and temperature variations of different components of solar collector.*

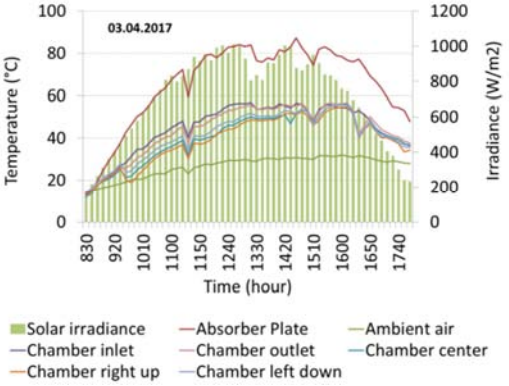

Figure 8. *Irradiance and temperature variations inside the chamber, absorber plate and ambient air with unload drying chamber.*

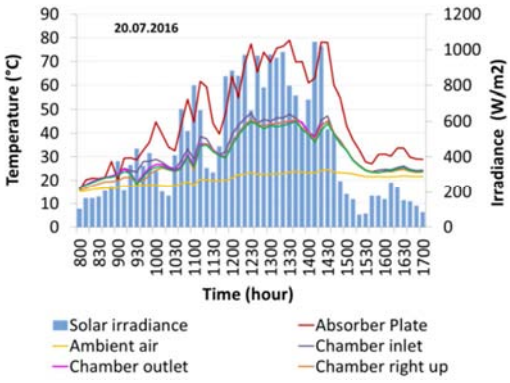

Figure 9. *Irradiance and temperature variations inside the chamber, absorber plate and ambient air during the drying of mushrooms.*

It has been observed that when the intensity of the radiation is high, there is a higher temperature gradient between the absorber plate and the air entering the drying camera regardless of whether it is without load or loaded with different products being dehydrated.

8.2. Moisture Content

The moisture content variation with drying time for apple is showed in figure 10. The drying curves were obtained from registered data on June 18, 2016 and February 23, 2017. The moisture content decreased exponentially with drying time which is reduced from 83% to about 10%. The

experimental results for February and June reveal that the apple slices attaint their equilibrium moisture content i.e. they are dehydrated in the solar drying in approximately 300 minutes. At the initial stage of drying curves, the heat transferred from the flowing air to the slice apples surface is used to evaporate the moisture from the surface of the product. In the next stage, the heat is transferred inside the product and hence the water as liquid or vapor is transported to the surface and from there is dragged by flowing air. Figure 11 shows the dimensionless parameter called moisture ratio versus drying time obtained to normalize the drying curves.

As expected, the drying curves are similar even when the solar radiation received was different as is shown in figure 12 and consequently reaching different temperatures inside the drying chamber (figure 13). The synthesis of the values of average irradiation, maximum irradiance and maximal temperature of hot air inside the drying chamber, absorber plate and ambient air are presented in table 1. On February 23 was received 9% more average irradiation and the maximal temperature in drying chamber was 3% less than on July 18 however, the trend of temperature curves inside the drying chamber from 10 a.m. to 2:30 p.m. is similar.

Table 1. *Maximal irradiance and temperatures on July 18 and February 23.*

DAY	Average Irradiation (kWh/m^2)	Maximal Irradiance (W/m^2)	Maximal Ambient Air Temp. (°C)	Maximal Absorber Plate Temp. (°C)	Maximal Drying chamber Temp. (|°C)
Jul. 18	5.6	1065	27.15	86.57	56.04
Feb. 23	6.1	1025	29.40	82.34	54.35

8.3. Thermal Images and Apple Slices Temperature

The apple temperature during drying process was monitored by IR thermography. The thermal images presented in figure 14 correspond to the product placed on the upper tray on December 7, 2016. The sequence shows four moments of drying process. The apple slices were introduced into the drying chamber at 10 a.m. The first thermal image (figure 14a) reveals that at 11 a.m. apple slices have a temperature between 28°C and 31°C when the air inside drying chamber has attained 51.27°C. The second (figure 14b) at 11:30 a.m. shows a temperature between 27°C and 29°C and the hot air temperature reached is 50.58°C. The third (figure 14c) at noon displays the slices of apple with a temperature between 30°C and 32°C and the flowing air temperature of 53.18°C.

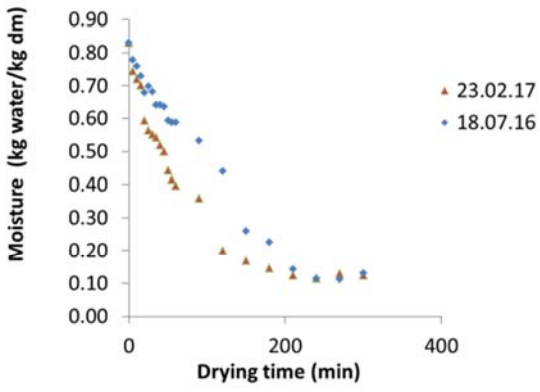

Figure 10. *Moisture content variation versus drying time.*

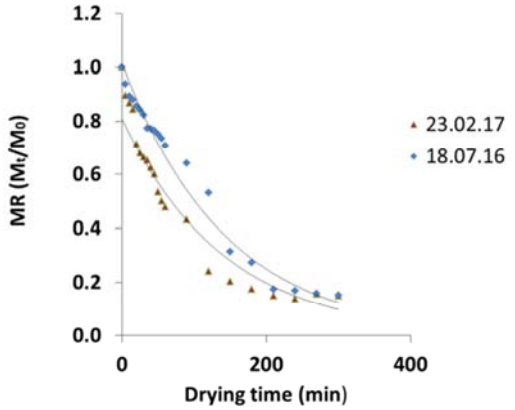

Figure 11. *Moisture ratio versus drying time.*

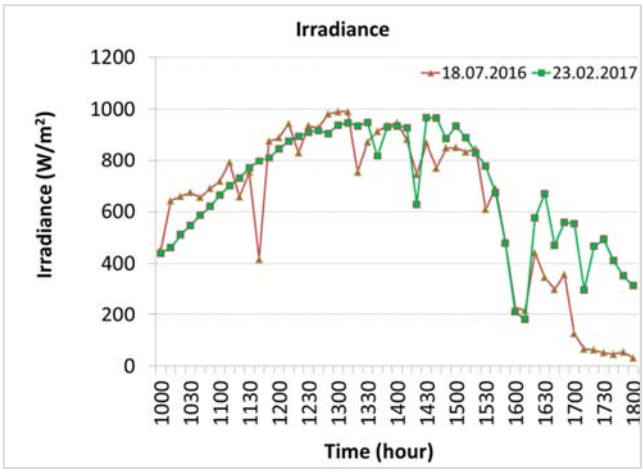

Figure 12. *Solar radiation on July 18 and February 23.*

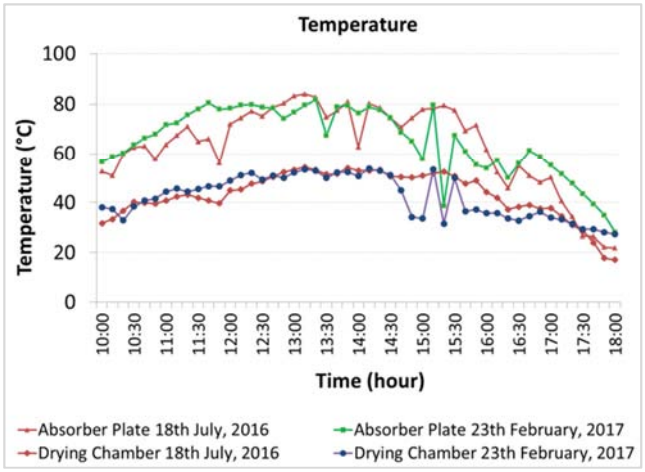

Figure 13. *Temperature variation for drying chamber and plate.*

The fourth (figure 14d) at 1:00 p.m. shows that apple has reached a temperature between 36°C and 37°C and the hot air 53.81°C. Figure 15 shows a thermal image sequence of the product deposited in three intermediate trays. The first thermal image (figure 15a) reveals that at 11:25 a.m. the apple slices have a temperature between 27°C and 30°C when the air inside the drying chamber has attained 50.58°C. The second (figure 15b) at 12:37 p.m. shows a temperature between 30.8°C and 34.5°C and the hot air temperature reached is 55.35°C. The third (figure 15c) at 1:15 p.m. displays the slices of apple with a temperature between 33°C and 34°C and the flowing air temperature is 53.18°C. The fourth (figure 15d) at 2:15 p.m. shows that apple has a temperature between 27°C and 28°C and the registered hot air temperature was 54.9°C. The data synthesis is shown in table 2 and figure 16.

Figure 17 shows the temperature gradients in each slice. Tenths of degree or even one entire degree in the temperature gradient are observed in the same slice and from 1-3 degrees among slices of a tray.

The maximal temperature reached by the absorber plate in the eleven months registered, was 89.42°C and 58.35°C for the air inside the chamber i.e. the air does not exceed a temperature of 60°C thereby is ensured that the products dehydrated will keep their nutrients undamaged.

Temperature gradients observed may be due to the position of the sun depending on the time and day since the drying chamber, even when it has thermal isolation, allows the solar radiation to penetrate and slightly increases the temperature of the east side in the mornings and the west side in the afternoons. In addition, the pipe of each side is undergone the same phenomenon. Thus, these two conditions are responsible for the increase of temperature gradient observed. Figure 17 shows the temperature gradients on June 18, 2016 at 11:00 a.m. The temperature on the east side is 28.7°C (right side in the picture) and 23.7°C on the west side. In the thermal image, it is observed that half of each tray has a temperature higher than 23.7°C.

Next to the thermography, from the simulation software PVSYST, is presented the image of the sun's position (red circle) with respect to the drying chamber and its chimney, for the same day and hour. Figure 18 shows what happens one hour later when the altitude of the sun is 88°. It is observed that there is a lower temperature gradient on the trays, and the region on each tray with lower temperature has been reduced. As sun's path changes, it is possible to reach a thermal equilibrium in the trays but later a gradient will be observed in which the west side will have a higher temperature than the east side. However, it should be noted that the temperature gradients of the apple slices are lower when the moisture content is also lower.

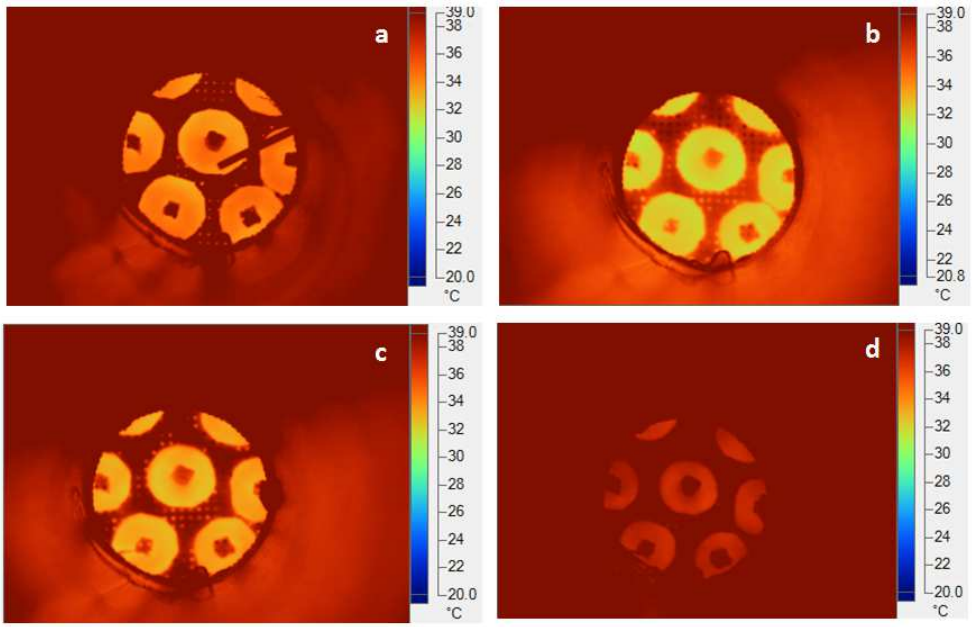

Figure 14. *Thermal images of the product placed on the upper tray.*

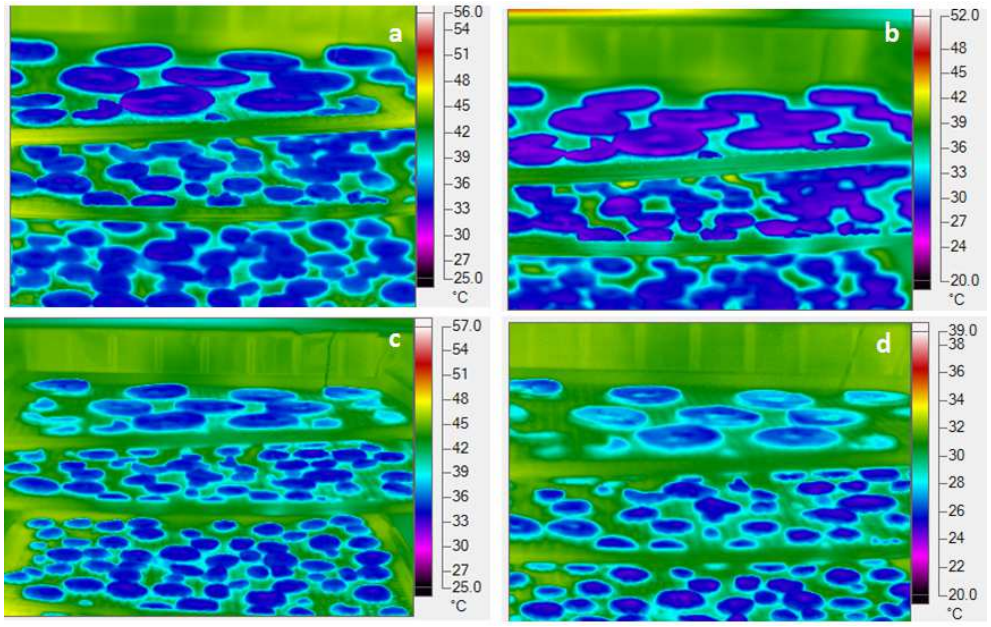

Figure 15. *Thermal images of apple slices during the drying process.*

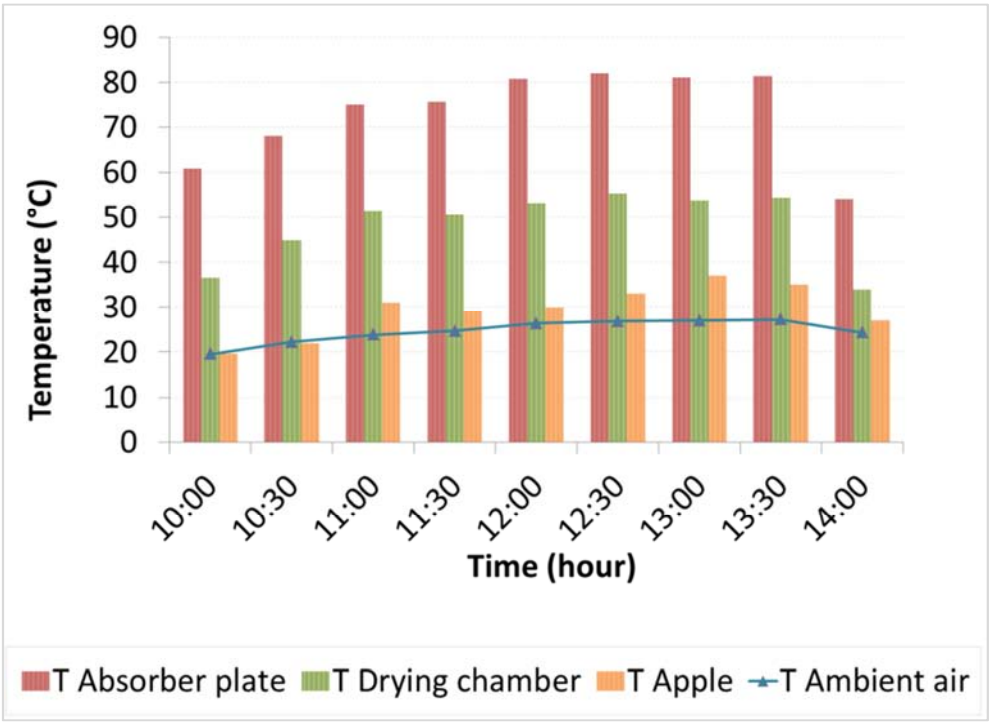

Figure 16. *Temperature variation of apple, solar dryer and ambient air.*

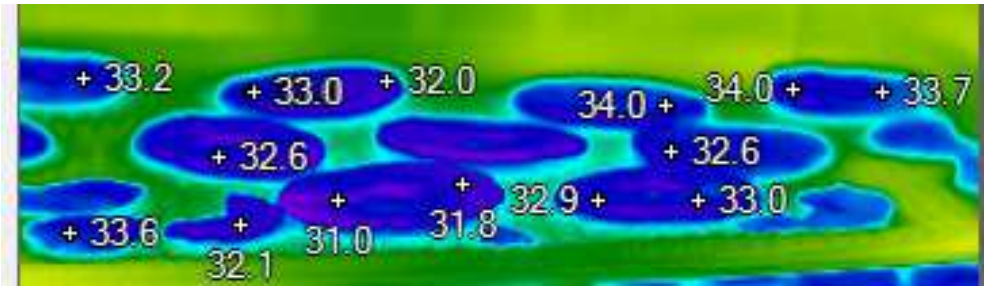

Figure 17. *Temperature gradients in each apple slice.*

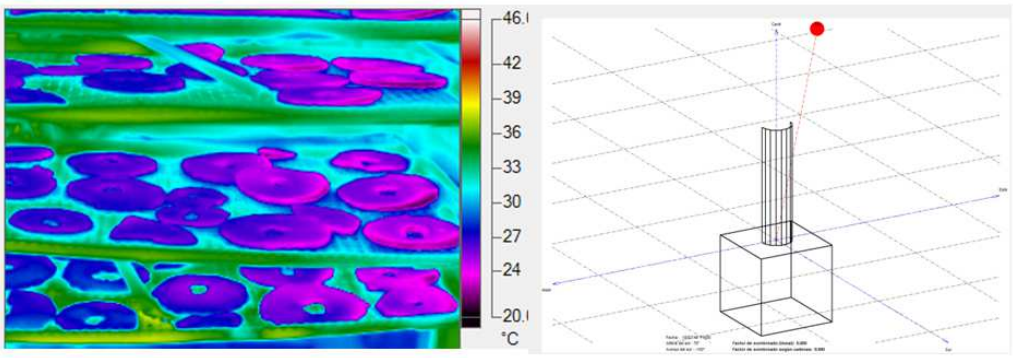

Figure 18. *Temperature gradients and sun's position on June 18, 2016 at 11:00 a.m.*

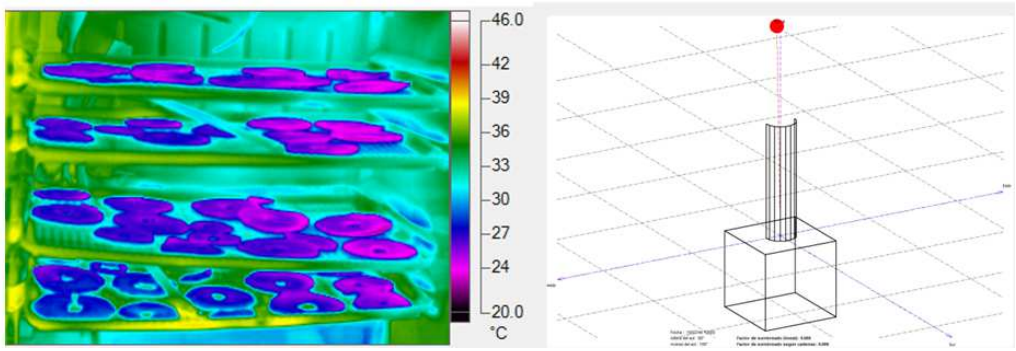

Figure 19. *Temperature gradients and sun's position on June 18, 2016 at 12 noon.*

Table 2. *Temperature variation of apple, solar dryer and ambient air on December 7, 2016.*

Hour	10:00	10:30	11:00	11:30	12:00	12:30	13:00	13:30	14:00
Plate	60.87	68.03	75.06	75.78	80.80	81.99	81.09	81.39	54.9
Chamber	36.48	44.84	51.27	50.58	53.18	55.35	53.81	54.35	33.88
Apple	19	21-22	29-31	27-29	30-32	32-33	36-37	33-34	25-27
Amb air	19.58	22.27	23.87	24.70	26.44	26.88	26.99	27.27	24.34

9. Conclusions

The proposed solar dryer prototype has been designed and constructed for drying agricultural products. The pipe design facilitates a homogeneous distribution of the drying air anywhere in the drying chamber.

Thermal performance inside the drying chamber makes it possible for the product placed in all trays to lose evenly the moisture.

The drying air temperatures inside the drying chamber are found in the range of 44-58.35°C which is suitable for drying the most agricultural products in one single day.

Thermal images are a useful tool in the drying process to visualize the thermal gradients, the maximal temperature reached and moisture presence in the product to be dehydrated.

The simplicity of the design of this solar collector allows farmers to construct it using local materials and common tools.

To promote the use of solar technology is a way to contribute to a sustainable development.

Acknowledgements

The authors would like to thank Dr. Juan José Santibañez for the financial support for the purchase of materials needed for the construction of this solar dryer and Dr. Juan José Ambriz García for lending us the infrared camera.

References

[1] Krokida, M. K., & Marinos-Kouris, D. "Rehydration kinetics of dehydrated products." Journal of Food Engineering, Volume 57(1), pp 1–7. March 2003.

[2] Tripaty, P. P. "Investigation into solar drying of potato: effect of simple geometry on drying kinetics and CO2 emissions mitigation." J Food Sci Technol. Volume 52(3), pp 1383-1393. March 2015.

[3] Gulcimen, F., Karakaya, H. and Durmus, A. "Drying of sweet basil with solar air collectors." Renewable Energy. Volume 93, pp 77-86. August 2016.

[4] Maskan, M. "Microwave/air and microwave finish drying of banana." Journal of Food Engineering. Volume 44, issue 2, pp 71–78. May 2000.

[5] Aguilera. J. M. "Drying and dried products under thE microscope." Food Sci. Tech. Int. Volume: 9 issue: 3, pp. 137-143, June 2003.

[6] Lin, T. M., Durance, T. D., & Scaman, C. H. "Characterization of vacuum microwave air and freeze dried carrot slices." Food Research International. Volume 4, pp 111–117. March 1998.

[7] Nindo, C., Sun, T., Wang, S. W., Tang, J. and Powers J. R. "Evaluation of drying technologies for retention of physical quality and antioxidants in asparagus. Leben Wissen Technol. Volume 36, pp 507-516. August 2003.

[8] Beaudry, C., Raghava, G., Ratti, C and Rennie, T. "Effect of four drying methods on the quality of osmotically dehydrated cranberries." Drying Technol Volume: 22, pp 521-539. February 2007.

[9] Leon, A., Kumar, M., and Bhattacharya, S. "A comprehensive procedure for performance evaluation of solar food dryers." Renewable and Sustainable Energy Reviews, Volume 6, issue 4, pp 367-393. August 2002.

[10] Bezyma LA, Kutovoy V. A. "Vacuum drying and hybrid technologies" Stewart Post- harvest Review. Volume 4, pp 6-13, December 2005.

[11] Kant, K., Shukla, A., Sharma, A., Kumar, A and Jain A. "Thermal energy storage based solar drying systems: A review." Innovative Food Science and Emerging Technologies. Volume 34, pp 86-99. April 2016.

[12] Gowen, A., Tiwari, B., Cullen, P., McDonnell, K. and O'Donnell, C. "Applications of thermal imaging in food quality and safety assessment." Trends in Food Science & Technology. Volume 21, pp 190-200. April 2010.

[13] Amon, F., Hamins, A., Bryner, N and Rowe, J. "Meaningful performance evaluation conditions for fire service thermal imaging cameras." Fire Safety Journal. Volume 43. Issue: 8, pp. 541-550, November 2008.

[14] Bagavathiappan, S., Lahiri B. B., Saravanan, T., Philip, J and Jayakumar, T. "Infrared thermography for condition monitoring. A review." Infrared Physics & Technology. Volume 60, pp 35-55. September 2013.

[15] Ridley, I. "Practical aspects of infrared remote thermometry. In Instrumentation and Sensors for the Food Industry" (E. Kress-Rogers and C. J. B. Brimelow, eds.) 187-212, CRC Press, Boca Raton, FL.

[16] Lidhoo C. K. and Agrawal Y. C. "Hot-air oven drying characteristics of button mushroom-safe drying temperature." Mush Res Vol. 15, pp 59-62. 2006.

[17] Mayor, L., Sereno, A. M. "Modelling shrinkage during convective drying of food materials." J Food Eng. Volume 61, pp 373-386. February 2004.

[18] Sagar, V. R. "Recent advances in drying and dehydration of fruits and vegetables: a review." J Food Sci Technol. Volume 47(1), pp 15-26. January 2010.